

# Embedded Model Predictive Control with Certified Real-Time Optimization for Synchronous Motors

Gionata Cimini, Daniele Bernardini, Stephen Levijoki, and Alberto Bemporad, *Fellow, IEEE*

**Abstract**—Model Predictive Control (MPC) is a very attractive candidate to replace standard field-oriented control algorithms for electrical motors. We demonstrate that it is possible to implement an MPC algorithm for Continuous Control Set (CCS-MPC), with both inputs and states constraints, in which the associated Quadratic Programming (QP) problem is solved online, even on the computationally limited platforms used in control of electrical motors. We detail the implementation of an active-set algorithm to solve efficiently the associated QP problem. Moreover, by exploiting recent results on active-set solver certification we are able to assess the computational complexity of the online optimization algorithm, providing the exact worst-case solution time. The controller is experimentally tested on an embedded control unit for the torque regulation of a permanent magnet synchronous motor, and benchmarked against explicit MPC. Computational feasibility, low-memory occupancy, and worst-case certification are achieved, fulfilling all the requirements of embedded control.

**Index Terms**—Model predictive control, electrical motors, torque control, synchronous drives, real-time optimization, quadratic programming, embedded control, complexity certification.

## I. INTRODUCTION

IMPROVING the performance of electrical systems is strategic in many applications, therefore Model Predictive Control (MPC) is a very active topic for power converters and drives control [1]–[4]. As far as transistor-based systems, the literature splits into Continuous Control Set (CCS)-MPC, which takes actions into a continuous set, corresponding to the modulator duty-cycle [5] and Finite Control Set (FCS)-MPC which instead manipulates directly the transistors [6], [7]. Recent research has compared the two strategies [8]–[10], with attempts to benefit from both [11]. FCS-MPC provides a faster response and possibly reduces the switching losses. However, the variable frequency increases components stress [12]–[14], and introduces a trade-off between tracking error, harmonics and energy efficiency [15]–[17].

CCS-MPC cancels the drawbacks associated with variable switching frequency, and provides decoupling between sampling and switching times [7], [18]. It is also the preferred choice when dealing with pre-compensated systems [19]. Unfortunately, the online optimization problem associated with constrained CCS-MPC, and non-trivial prediction horizon, is typically considered unmanageable on low-cost platforms [20].

G. Cimini and D. Bernardini are with ODYS Srl, 20159 Milano, Italy, (e-mail: gionata.cimini@odys.it; daniele.bernardini@odys.it).

S. Levijoki is with General Motors Company, Detroit, MI, USA, (e-mail: stephen.levijoki@gm.com).

A. Bemporad is with IMT School for Advanced Studies Lucca, 55100 Lucca, Italy, and ODYS Srl, (e-mail: alberto.bemporad@imtlucca.it).

Computational burden has been an issue for FCS-MPC too, but recently the combinatorial complexity has been severely reduced [21], [22], with a consequent gain in its popularity. The goal of this paper is to demonstrate that recent advances in convex optimization make CCS-MPC feasible on cheap hardware as well, providing in addition an analytical bound to its complexity [23]. The alternative to online optimization would be explicit MPC (EMPC), which pre-solves the optimization problem offline [24]. However, the logarithmic search time and polynomial memory occupancy make EMPC feasible only for small problems, with few inputs and a short horizon. Successful applications of EMPC for electrical motors hold only for simplified formulations, one-step ahead prediction and/or approximated constraints [25], [26].

This paper presents a CCS-MPC algorithm based on online optimization for the torque tracking of a Permanent Magnet Synchronous Motor (PMSM), that we refer to as Model Predictive Torque Control (MP-TC). We demonstrate that it is possible to efficiently solve the Quadratic Programming (QP) problem arising in linear MPC on a platform with scarce computational capabilities. To the best of the authors' knowledge, online CCS-MPC for motor control and embedded in a low-cost platform has been investigated only in [27], [28]. However, in [27] the input constraints are not present, and the quality of the obtained solution is not discussed. The authors have considered input constraints in [28], but the control performance and computational feasibility have been assessed only with hardware-in-the-loop, and the worst-case run time for the solver is unknown. This paper considers an experimental setup, where the optimal control sequence is computed by an embedded active-set solver. Such optimization methods achieve very high accuracy in a fixed amount of iterations, even under single-precision arithmetic.

As a further contribution, we certify analytically the worst-case execution time of the optimization. With embedded MPC becoming increasingly popular in industry, see for instance the mass production of General Motors [29], [30], complexity certification is of paramount importance. Namely one has to prove that the inputs will be always computed in a time interval that is smaller than the sampling one [31]. Active-set methods have suffered for a while from the lack of such theoretical bounds, despite the experimental evidence of an average polynomial complexity. The authors have solved this issue in [23] by demonstrating that the iterations taken by a dual active-set method when solving a parametric QP problem depend in a piecewise affine (PWA) fashion on the vector of parameters. Therefore, we are able to compute exactly the number of floating-point operations (flops) needed in the worst-case to

solve the optimization problem. A block principal pivoting method has been proved to enjoy similar properties [32] while being faster, however the need to impose constraints on the motor currents restricts the choice to algorithms that can handle general inequality constraints, i.e. [23].

The proposed MP-TC has been tested on a commercially available PMSM, controlled by a Texas Instruments<sup>®</sup> DSP, commonly used in power electronics and electrical drives. The comparison with EMPC is also shown, being the only valuable alternative to meet embedded requirements for a CCS-MPC algorithm. The results show that the proposed MP-TC highly reduces the memory occupancy and, more interestingly, it requires a lower worst-case number of flops when compared to EMPC, increasing the throughput.

The paper is organized as follows. Section II derives the mathematical model of the PMSM, and the MP-TC algorithm is presented in Section III. The embedded solver design and certification are detailed in Section IV, and the experimental results reported in V. Finally, Section VI concludes the paper.

## II. MATHEMATICAL MODEL

The electrical subsystem of a PMSM is modeled with respect to the  $(d, q)$  reference, frame rotating synchronously with the rotor

$$\dot{i}_d(t) = -\frac{R}{L_d}i_d(t) + \frac{L_q}{L_d}\omega(t)i_q(t) + \frac{1}{L_d}u_d(t) \quad (1a)$$

$$\dot{i}_q(t) = -\frac{R}{L_q}i_q(t) - \left(\frac{L_d}{L_q}i_d(t) + \frac{\lambda}{L_q}\right)\omega(t) + \frac{1}{L_q}u_q(t) \quad (1b)$$

where  $t \in \mathbb{R}_+$  is the time index,  $d$  and  $q$  are the subscripts for *direct* and *quadrature* quantities,  $L$ ,  $R$ ,  $i$  and  $u$  are the stator inductance [H], resistance [ $\Omega$ ], current [A] and voltage [V]. The mechanical dynamics of a PMSM are as follows:

$$\dot{\omega}(t) = \frac{B}{J}\omega(t) + \frac{p}{J}\tau(t) - \frac{p}{J}\tau_l(t) \quad (2a)$$

$$\tau(t) = \frac{3}{2}p(\lambda i_q(t) + (L_d - L_q)i_d(t)i_q(t)) \quad (2b)$$

where  $\omega(t)$  is the electrical rotor speed [rad/s],  $\tau(t)$  is the electrical torque [Nm],  $J$  is the inertia coefficient [kg·m<sup>2</sup>],  $\lambda$  is the motor flux leakage [Wb],  $\tau_l(t)$  is the load torque [Nm], and  $p$  is the number of pole pairs. Let us assume that the PMSM is isotropic with  $L_d \equiv L_q \equiv L$  and nominal speed  $\omega_0$ , and let  $K_t = \frac{3}{2}p\lambda$  be the torque constant. Define the states  $x(t) = [i_d(t), i_q(t)]'$ , the manipulated inputs  $u(t) = [u_d(t), u_q(t)]'$ , the measured outputs  $y(t) = [i_d(t), \tau(t)]'$  and the measured disturbances  $v(t) = \omega(t)$ . Then, the following Linear-Time-Invariant (LTI) model defines an approximation of the electrical subsystem (1):

$$\begin{aligned} \dot{x}(t) &= \underbrace{\begin{bmatrix} -\frac{R}{L} & \omega_0 \\ -\omega_0 & -\frac{R}{L} \end{bmatrix}}_{A_c} x(t) + \underbrace{\begin{bmatrix} \frac{1}{L} & 0 \\ 0 & \frac{1}{L} \end{bmatrix}}_{B_c} u(t) + \underbrace{\begin{bmatrix} 0 \\ \lambda \\ -\frac{1}{L} \end{bmatrix}}_{G_c} v(t) \\ y(t) &= \underbrace{\begin{bmatrix} 1 & 0 \\ 0 & K_t \end{bmatrix}}_{C_c} x(t) \end{aligned} \quad (3)$$

Such model is obtained by imposing a nominal speed in the terms  $\omega(t)i_q(t)$  and  $\omega(t)i_d(t)$ , while allowing the flexibility of having time-varying values in the affine term  $v(t)$ . This improves the accuracy of the model with respect to more conservative approaches where the effect of the speed is completely linearized around a steady-state value [27].

## III. MODEL PREDICTIVE CONTROL DESIGN

Standard PI-FOC consists of a cascaded architecture where the outer loop regulates either the rotor speed or position, and the inner loop controls the  $(d, q)$  stator currents, see Figure 1. MP-TC replaces the controller of the electrical subsystem, keeping the external loop unchanged, see Figure 2. The focus on the inner loop is motivated by the faster dynamics, and by the necessity to impose voltage and current constraints. In an not weakening flux operation, the direct component  $i_d$  has to be stabilized at zero, while the quadrature component  $i_q$  has to track the set-point  $i_q^{\text{ref}}$ , obtained by scaling the torque reference  $\tau^{\text{ref}}$  by the constant  $K_t$ . With isotropic machines this control algorithm is effective, as maximum current implies maximum torque. However, in order to tackle field weakening, Maximum Torque per Ampere (MTPA) could be considered [7], [27], but that is out of the scope of this paper.

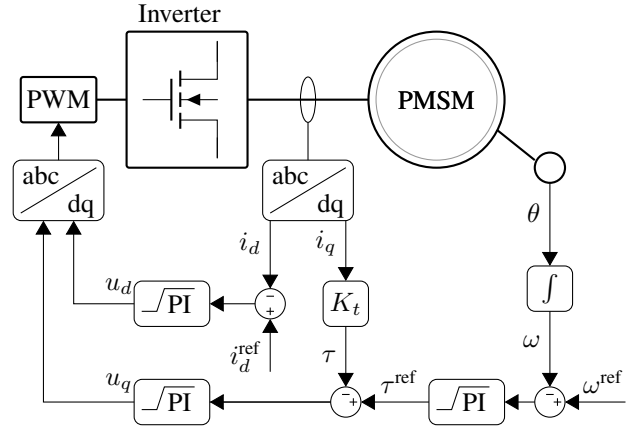


Figure 1. Standard field oriented control scheme for a PMSM. Both the speed loop and the two stator currents loops are controlled by linear regulators.

### A. MPC formulation

Linear MPC solves a finite-horizon, constrained, optimal control problem, based on a linear prediction model obtained by discretizing (3) with sampling time  $T_s$ , such that:

$$\begin{aligned} x(k+1) &= Ax(k) + Bu(k) + Gv(k) \\ y(k) &= Cx(k) \end{aligned} \quad (4)$$

where  $k \in \mathbb{N}$  is the discrete-time index,  $A = e^{A_c T_s}$ ,  $B = \int_0^{T_s} e^{A_c \tau} d\tau B_c$ ,  $G = \int_0^{T_s} e^{A_c \tau} d\tau G_c$ , and  $C = C_c$ . The goal is to track the reference  $\tau^{\text{ref}}$  while constraining voltages

and currents. Therefore the following optimization problem is solved at every time step  $k$

$$\min_{\Delta \bar{u}} \sum_{i=1}^{N_p} \|W_y(y_{k+i|k} - r(k))\|_2^2 + \sum_{j=0}^{N_u-1} \|W_{\Delta u} \Delta u_{k+j|k}\|_2^2 \quad (5a)$$

$$\text{s.t. } x_{k|k} = x(k), \quad (5b)$$

$$x_{k+i+1|k} = Ax_{k+i|k} + Bu_{k+i|k} + Gv(k), \quad (5c)$$

$$y_{k+i+1|k} = Cx_{k+i+1|k}, \quad (5d)$$

$$\Delta u_{k+N_u+j|k} = 0, \quad j = 0, \dots, N_p - N_u - 1 \quad (5e)$$

$$u_{k+i|k} \in \mathbb{U}, \quad (5f)$$

$$x_{k+i+1|k} \in \mathbb{X}, \quad (5g)$$

$$i = 0, 1, \dots, N_p - 1 \quad (5h)$$

where  $\Delta \bar{u} = \{\Delta u_{k|k}, \dots, \Delta u_{N_u-1|k}\}$  is the sequence of input increments, and  $\Delta u_{k+i|k} = u_{k+i|k} - u_{k+i-1|k}$ ,  $i = 0, 1, \dots, N-1$ , with  $u_{k-1|k} = u(k-1)$ . In Equation (5)  $N_p$  and  $N_u$  are the prediction and control horizons, and  $r(k) = [0, \tau^{\text{ref}}(k)]'$ ,  $x_{k+i|k}$  denotes the prediction of the variable  $x$  at time  $k+i$  based on the information available at time  $k$ ,  $W_y$  and  $W_{\Delta u}$  are weight matrices of appropriate dimensions. Inputs and states constraints are imposed by Equations (5f)-(5g), respectively, where  $\mathbb{U}$  and  $\mathbb{X}$  are polyhedral sets defined in Section III-B.

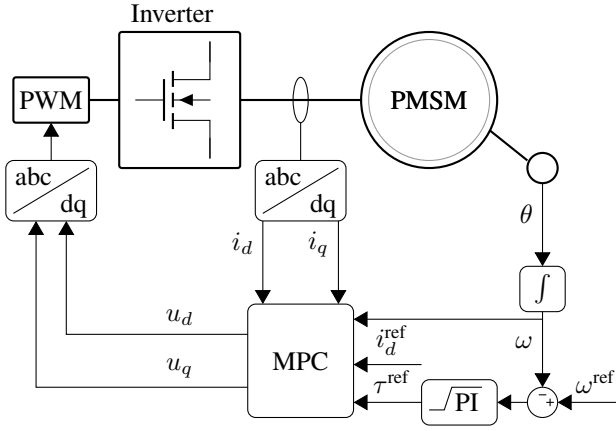


Figure 2. The proposed control scheme for PMSM. The speed loop is controlled by a standard regulator, the inner loop is implements the model predictive torque control here introduced.

### B. Constraints

We need to impose constraints on stator voltages and currents [33]. Specifically, the inverter imposes a phase voltage limit linked to the modulation scheme. Given a DC-bus voltage  $V_{\text{DC}}$ , such limit is set to  $V_{\text{max}} = \frac{V_{\text{DC}}}{\sqrt{3}}$  for both space-vector and pulse-width modulations [27]. The maximum stator current  $I_{\text{max}}$  is imposed to prevent overheating, and their violation for short intervals due to constraints' softening of (5g) is usually permitted. Such bounds get transformed into norm constraints in the  $(d, q)$  reference frame, such as:

$$u \in \tilde{\mathbb{U}} = \{u \in \mathbb{R}^2 : \|u\|_2 \leq V_{\text{max}}\} \quad (6a)$$

$$x \in \tilde{\mathbb{X}} = \{x \in \mathbb{R}^2 : \|x\|_2 \leq I_{\text{max}}\}. \quad (6b)$$

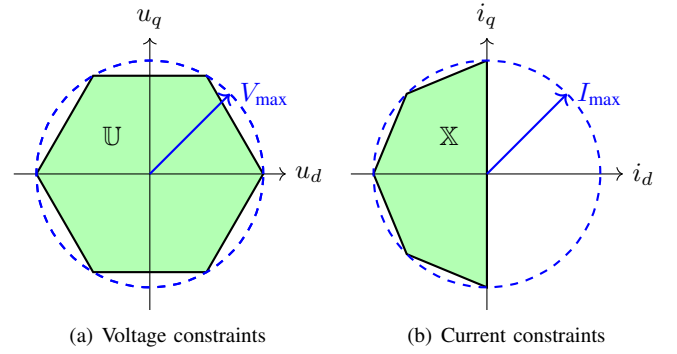


Figure 3. Inputs (a) and outputs (b) constraints imposed by the MPC controller. The blue circles represent the original norm constraints of Eq. (6). The green regions represent their approximations, and are the polyhedra described by the sets  $\mathbb{U}$  and  $\mathbb{X}$ , respectively.

A polytopical approximation of the quadratic constraints (6) helps reducing the complexity of the optimization problem [25], [27], and in this paper we approximate the feasible regions as in Figure 3, which results into an acceptable trade-off between the accuracy and number of inequality constraints.

### C. State estimation and integral action

Although all states are measured for this application, the controller takes advantage of an observer to reduce the impact of measurements noise, e.g. due to transistor switching. A Kalman filter is employed to mitigate such noise, using the state estimation  $\hat{x}_{k|k}$  instead of the measured state  $x(k)$  in (5b). We introduce a delay of one time step in the input channel to account for the time spent in computing the optimal control move. Let  $L$  be the Kalman filter gain, the one-step delayed implementation is achieved by computing the state estimate as

$$\hat{x}_{k+1|k} = (A - LC)\hat{x}_{k|k-1} + Bu_{k-1} + G_v v_k + Ly_k. \quad (7)$$

Integral action is added to the torque reference to minimize tracking error, therefore dealing with model uncertainties and noise. That allows us to reject constant disturbances without affecting the optimization problem size. The modified torque reference is denoted by  $\tilde{y}^{\text{ref}} = [\tilde{i}_d^{\text{ref}}, \tilde{\tau}^{\text{ref}}]'$  and computed as:

$$\tilde{i}_d^{\text{ref}}(k) = \tilde{i}_d^{\text{ref}}(k-1) + k_1(i_d^{\text{ref}}(k) - i_d(k)) \quad (8a)$$

$$\tilde{\tau}^{\text{ref}}(k) = \tilde{\tau}^{\text{ref}}(k-1) + k_2(\tau^{\text{ref}}(k) - \tau(k)) \quad (8b)$$

where  $k_1, k_2$  are scalar parameters. Figure 4 shows the complete real-time MPC controller scheme.

## IV. ONLINE OPTIMIZATION AND COMPLEXITY CERTIFICATION

Let us rewrite (5) as a the following parametric QP problem:

$$\begin{aligned} \min_z \quad & \frac{1}{2} z' H z + \theta_k' F' z \\ \text{s.t.} \quad & G z \leq S \theta_k + s \end{aligned} \quad (9)$$

where  $z = [\Delta \bar{u}' \quad \rho']' \in \mathbb{R}^{n_z}$  is the vector of optimization variables, collecting the sequence of input increments  $\Delta \bar{u}$  and the vector  $\rho$  of slack variables used for softening state constraints,  $\theta_k \in \Theta \in \mathbb{R}^{n_\theta}$  is the vector of parameters

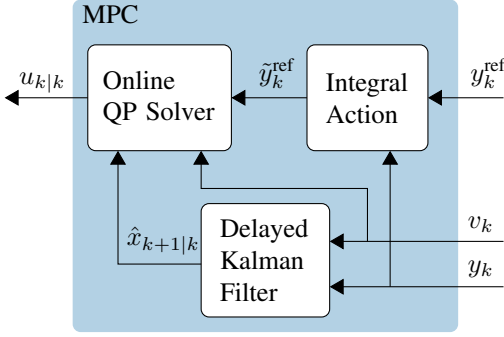


Figure 4. Block scheme of the MPC controller, with delayed Kalman filter for state estimation, integral action for offset-free tracking and the online solver to obtain the inputs- sequence.

defined as  $\theta_k = [u'_{k-1}, \hat{x}'_{k+1|k}, r'_k, v'_k]'$ , with  $\Theta$  a set of interest,  $H \in \mathbb{R}^{n_z \times n_z}$  is a symmetric and positive definite matrix,  $F \in \mathbb{R}^{n_z \times n_\theta}$ ,  $G \in \mathbb{R}^{m_z \times n_z}$ , and  $S \in \mathbb{R}^{m_z \times n_\theta}$  and  $s \in \mathbb{R}^{m_z}$ . Solving (9) accurately and with a throughput in the milliseconds scale is challenging on embedded hardware. One option could be EMPC, in which the QP is solved offline for all  $z$ , and the optimal control law is obtained via multiparametric programming [24]. However, EMPC is less attractive when the number of regions of the resulting PWA controller grows, as it could require a significant amount of memory. Indeed, in the next section we show that the memory occupancy of EMPC would be too high for this application.

In this work we implemented an efficient QP solver based on an active-set method, that will be shown to solve problem (9) within the allowed time limit, and with an exact assessment of the worst-case execution time.

#### A. Active-set solver

**Definition IV.1 (Active set).** Given a QP problem as in (9), a constraint is said to be *active* at  $\bar{z}$  if it is satisfied as equality constraint, i.e.,  $G_i \bar{z} = S_i \theta_k + s_i$ , where  $A_i$  represents the  $i$ -th row of a matrix  $A$ , and  $a_i$  represents the  $i$ -th element of a vector  $a$ . Otherwise, it is *inactive*. We define the two sets

$$\mathcal{A}(\bar{z}) = \{i \in \mathcal{K} \mid G_i \bar{z} = S_i \theta_k + s_i\} \quad (10a)$$

$$\mathcal{I}(\bar{z}) = \{i \in \mathcal{K} \mid G_i \bar{z} < S_i \theta_k + s_i\} \quad (10b)$$

where  $\mathcal{K} = \{1, \dots, m\}$  collects the constraint indexes,  $\mathcal{A}$  is the *active set* and  $\mathcal{I}$  the *inactive set*, such that  $\mathcal{I} = \mathcal{K} \setminus \mathcal{A}$ . ■

Given  $\mathcal{A}^*$  the set of constraints active at the optimal solution  $z^*$ , the idea behind active-set methods is to iteratively update the optimal constraints guess  $\mathcal{A}^j$ , known as *working-set*, until  $\mathcal{A}^j \equiv \mathcal{A}^*$  is verified. Let  $\mathcal{B}^j$  indicate the set of *blocking constraints*, namely those that prevent a full step in the primal space without violating dual feasibility. Then, at each iteration  $j$  a constraint  $v^j \in \mathcal{V}^j \subseteq \mathcal{I}$  is selected, with  $\mathcal{V}^j$  being the set of all the violated constraints, such that  $\mathcal{A}^j = \{\mathcal{A}^{j-1} \cup v^j\} \setminus \mathcal{B}^j$ . A step towards the optimal solution is obtained by solving the reduced equality-constrained QP problem

$$\begin{aligned} z^j &= \arg \min_z \frac{1}{2} z' H z + \theta'_k F' z \\ \text{s.t.} \quad & G_{\mathcal{A}^j} z = S_{\mathcal{A}^j} \theta_k + s_{\mathcal{A}^j}. \end{aligned} \quad (11)$$

#### Algorithm 1 Dual active-set solver

**Input:** Matrices  $H, F, G, S, s$  of problem (9), vector of parameters  $\theta_k$  and set  $\mathcal{K}$

- 1:  $z^0 \leftarrow -H^{-1} F \theta_k, \pi^0 \leftarrow 0, j \leftarrow 0, \mathcal{A}^{j-1} \leftarrow \emptyset;$
- 2:  $\mathcal{V}^0 \leftarrow \{i \in \mathcal{K} \mid G_i z^0 > S_i \theta_k + s_i\};$
- 3: **while**  $\mathcal{V}^j \neq \emptyset$  **do**
- 4:    $v^j \leftarrow \arg \max \{G_i z^j - S_i \theta_k - s_i, \forall i \in \mathcal{V}^j\};$
- 5:    $j \leftarrow j + 1;$
- 6:   Find blocking constraints  $\mathcal{B}^j;$
- 7:    $\mathcal{A}^j \leftarrow \{\mathcal{A}^{j-1} \cup v^j\} \setminus \mathcal{B}^j;$
- 8:   Solve  $\text{KKT}(\mathcal{A}^j)$  with respect to  $(z^j, \pi^j);$
- 9:    $\mathcal{V}^j \leftarrow \{i \in \mathcal{K} \mid G_i z^j > S_i \theta_k + s_i\};$
- 10: **end while**

**Output:** Optimal solution  $z^* = z^j$  and active set  $\mathcal{A}^* = \mathcal{A}^j$

Problem (11) amounts to find a primal-dual pair  $(z^j, \pi^j_{\mathcal{A}^j})$  that solves the Karush-Kuhn-Tucker (KKT) system

$$\text{KKT}(\mathcal{A}^j) \begin{bmatrix} H & G'_{\mathcal{A}^j} \\ G_{\mathcal{A}^j} & 0 \end{bmatrix} \begin{bmatrix} z^j \\ \pi^j \end{bmatrix} = \begin{bmatrix} -F \theta_k \\ S_{\mathcal{A}^j} \theta_k + s_{\mathcal{A}^j} \end{bmatrix} \quad (12)$$

with  $\pi = [\pi'_{\mathcal{A}^j} \quad \pi'_{\mathcal{I}^j}]'$  and  $\pi_{\mathcal{I}^j} = \mathbf{0}$ . The set  $\mathcal{B}^j \subseteq \mathcal{A}^{j-1}$  is composed by all those constraints that would prevent to solve the system  $\text{KKT}(\{\mathcal{A}^{j-1} \cup v^j\})$  without incurring in dual infeasibility, and that have to be dropped from the current working-set. Algorithm 1 describes the pseudo-code of the implemented dual active-set solver, which starts from the unconstrained solution  $H^{-1} F \theta_k$  and iterates towards primal feasibility by adding the most violated constraint at each iteration, preserving dual feasibility. If  $z^j$  is primal feasible, that is  $G_i z^j \leq S_i \theta_k + s_i, \forall i \in \{1, \dots, m\}$ , then  $z^j \equiv z^*$  holds [34]. Dual active-set solvers are preferable to primal ones because at the price of infeasible sub-iterates, they do not require *Phase I* to find a feasible initial guess and usually find the optimizer with less iterations [35].

#### B. Complexity certification of the dual active-set algorithm

Knowing the computational complexity of the controller is of highest importance in embedded real-time systems, in order to ensure that the control routine is always performed within the sampling time. The interest in certifying QP solvers is a very recent matter, as a consequence of the interest in embedded applications for MPC [23], [31]. The authors have introduced in [23] the theory and methods to compute exactly the worst-case execution time of a dual active-set solver, such as Algorithm 1, when solving a QP problem with the linear term of the cost function and right hand side of the constraints depending linearly on a vector of parameters as in (9). The objective of the certification algorithm is to exactly compute the maximum number of flops  $\mathcal{F}^{\max}$  performed by Algorithm 1 when solving problem (9) for any  $\theta_k \in \Theta$ , in order to guarantee that  $t(\mathcal{F}^{\max}) < T_s$ , where  $t(\mathcal{F})$  is the time needed by the selected processor to perform  $\mathcal{F}$  flops. The core result behind the certification algorithm is summarized by the following lemma.

**Lemma IV.1.** Let  $\Theta \subseteq \mathbb{R}^{n_\theta}$  be a polyhedron and  $z^0, \pi^0$  two affine functions of  $\theta \in \Theta$ , then for each iteration  $j \in \mathbb{N}$  of Algorithm 1 the primal-dual pair  $(z^j, \pi^j)$  obtained by solving KKT( $\mathcal{A}^j$ ) is PWA, and  $N : \Theta \rightarrow \{0, \dots, N^{\max}\}$  is an integer piecewise constant function, with  $N^{\max} = \max_{\theta \in \Theta} N(\theta)$  the maximum number of iterations performed for all  $\theta \in \Theta$ .

*Proof.* The reader is referred to [23, Theorem IV.4].  $\square$

Given the result of Lemma IV.1 it is possible to certify Algorithm 1 by iteratively splitting  $\Theta$  into polyhedral sub-regions according to the possible constraints added and dropped at each iteration. The polyhedra generated in this way at a given iteration  $j$  represent regions of the parameter space where the solution can be either optimal, infeasible, or requiring further iterates. Let us define the PWA primal dual pair as

$$z^j(\theta_k) = A_z^j \theta_k + b_z^j \quad (13a)$$

$$\pi^j(\theta_k) = A_\pi^j \theta_k + b_\pi^j \quad (13b)$$

with  $A_z^0 = -H^{-1}F$ ,  $b_z = \mathbf{0}^{n_z}$ ,  $A_\pi^0 = \mathbf{0}^{m_z \times n_\theta}$  and  $b_\pi^0 = \mathbf{0}^{m_z}$ . Then  $z^0$  and  $\pi^0$  are affine functions of  $\theta$  and the certification algorithm builds a set  $\mathbb{T}_{\text{opt}}$  of optimal tuples, and a set  $\mathbb{T}_{\text{inf}}$  of infeasible ones, where the generic tuple  $T^i$  is uniquely defined by the following parameters:

$$T^i = (\Theta^i, \mathcal{F}^i, j, \mathcal{A}^i, A_z^i, b_z^i, A_\pi^i, b_\pi^i). \quad (14)$$

It is therefore possible to certify the worst-case complexity by computing  $\mathcal{F}^{\max} = \max(\mathcal{F}_{\text{opt}}^{\max}, \mathcal{F}_{\text{inf}}^{\max})$ , where  $\mathcal{F}_{\text{opt}}^{\max}$  and  $\mathcal{F}_{\text{inf}}^{\max}$  are the number of flops needed in the worst-case to reach the optimum and to detect infeasibility, computed as:

$$\mathcal{F}_{\text{opt}}^{\max} = \max_{T \in \mathbb{T}_{\text{opt}}} \{\mathcal{F}(T)\} \quad (15a)$$

$$\mathcal{F}_{\text{inf}}^{\max} = \max_{T \in \mathbb{T}_{\text{inf}}} \{\mathcal{F}(T)\} \quad (15b)$$

where  $\mathcal{F}(T)$  denotes the value  $\mathcal{F}$  associated to the tuple  $T$ . The certification is also useful to identify if there is any region in the parameters' space where the QP algorithm would fail due to problem infeasibility. Moreover, the explicit solution can be easily obtained as a by-product of the certification algorithm [23], given that for each tuple we know the active constraints and the piecewise functions (13). Such feature will be exploited in the next section to compare the embedded QP solver with respect to its corresponding explicit version.

## V. EXPERIMENTAL RESULTS

The proposed MP-TC algorithm with real-time optimization has been tested on the commercially available MBE.300.E500 PMSM, by Technosoft SA. The control unit is an F28335 Delfino DSP by Texas Instruments, which belongs to the C2000 series. It has a 32-bit, 150 MHz CPU (6.67ns cycle time) and an IEEE-754 single-precision Floating-Point Unit, with an integrated multiplier (32 × 32 bit). This hardware has been chosen to demonstrate the viability of implementing an online QP solver in a low-cost platform like one of the C2000 family, which is commonly used in motion control.

The motor specifications are listed in Table I. The control scheme of Figure 4 and the QP solver have been implemented in C code to maximize efficiency. Two interrupt levels manage

Table I  
TECHNOSOFT MBE.300.E500 PMSM PARAMETERS

Parameter	Units	Value
Phase-phase resistance	ohm	8.61
Phase-phase inductance	mH	07.13
Back-EMF constant	V/1000 rpm	3.86
Torque constant	mNm/A	36.8
Pole pairs	–	1
Rated voltage	V	36
Max. voltage	V	58
No-load current	mA	73.2
No-load speed	rpm	9170
Max. cont. current (at 5000 rpm)	mA	913
Max. cont. torque (at 5000 rpm)	mNm	30
Max. permissible speed	rpm	15000
Peak torque (stall)	mNm	154
Rotor inertia	kgm <sup>2</sup> · 10 <sup>-7</sup>	11
Mechanical time constant	ms	7

Table II  
DESIGN PARAMETERS OF MP-TC

Prediction horizon $N_p$	3
Control horizon $N_u$	1
Voltage limit $V_{\max}$	24/√3 V
Current limit $I_{\max}$	1 A
Output weights $W_y$ and $P$	$\begin{bmatrix} 1 & 0 \\ 0 & 1 \end{bmatrix}$
Input increments weights $W_{\Delta u}$	$\begin{bmatrix} 0.01 & 0 \\ 0 & 0.01 \end{bmatrix}$
Sampling time $T_s$	0.3 ms

the controller scheduling: (i) a fast loop for current control with 0.3ms sampling time, and (ii) a slow loop for speed control with 1.2ms sampling time. The main design parameters of the MP-TC are summarized in Table II. In the next the so designed controller will be referred to as *implicit MP-TC*, and later compared to *explicit MP-TC* for which the online optimization is replaced by EMPC.

The certification algorithm described in Section IV-B has been applied to the MPC setup of Table II, in order to compute the worst-case behavior of the solver, and thus validate off-line the controller's complexity feasibility. The set  $\Theta$  has been derived in accordance with the physical constraints collected in Table I. Figure 5 shows a 2D projection in the parameter space of the optimal polyhedra corresponding to the tuples  $T^i \subseteq \mathbb{T}_{\text{opt}}, \forall i = 1, \dots, \text{card}(\mathbb{T}_{\text{opt}})$ . The same color means the same number of iterations performed by the solver, but with possibly different number of flops due to a different sequence of constraints added or removed from the active set. The algorithm certifies that  $\mathbb{T}_{\text{inf}} = \emptyset$  which guarantees that the solver is never infeasible on the set  $\Theta$ , and that the worst-case number of flops required by the implicit MP-TC controller is  $\mathcal{F}_I^{\max} = 2431$ , among which 10 are square roots. The memory occupation  $m_I$  of both code and data is computed to be 12.7kB which is well below the single-access RAM block of 34kB provided by the F28335. The desired rotor speed  $\omega^{\text{ref}}$  and the achieved speed  $\omega$  are shown in Figure 6. Abrupt changes of speed are requested in order to operate the system close to the constraints, therefore stressing the QP solver for speed evaluation. Figure 7 shows the stator currents in the  $(d, q)$  reference frame and the corresponding three phase

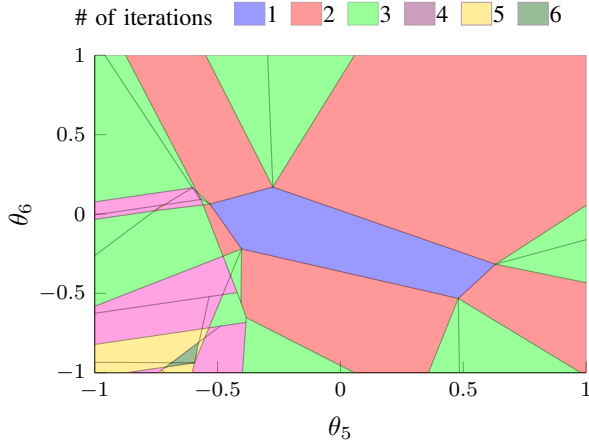


Figure 5. 2-D projection of the certification algorithm result over the plane defined by QP parameters  $p_5 \equiv i_d^{\text{ref}}$  and  $p_6 \equiv i_q^{\text{ref}}$ . Polyhedral regions with the same color share the same number of iterations, but possibly different flops to reach the optimum.

currents. Figure 8 presents the  $(d, q)$  stator voltages together with the corresponding three phase variables. As shown, the system constraints are correctly handled. Figure 9 shows the task times obtained by means of a high precision internal clock, and the number of iterations needed by the solver to obtain the optimal control sequence. The solution is always computed within the time limit of 0.3 ms. This time includes ADC sampling, state estimation, and real-time optimization.

The proposed implicit MP-TC is compared to explicit MP-TC. For a more comprehensive benchmark, two configurations have been proposed. *Setup 1* is the one discussed above, whereas *Setup 2* denotes a simplified version with the polyhedral constraints on the currents replaced by box constraints in the  $(d, q)$  frame, similarly to [25], such that:

$$i_d \in [-\epsilon I_{\max}, \epsilon I_{\max}] \quad (16a)$$

$$i_q \in [I_{\max}, I_{\max}] \quad (16b)$$

with  $\epsilon > 0$ . The flops and memory occupancy of explicit MP-TC, respectively identified by  $\mathcal{F}_E^{\max}$  and  $m_E$ , are obtained by considering the implementation described in [36, Algorithm 4]. For each of the two controller setups, different prediction horizons are also considered, and the complete benchmark is summarized in Table III, where  $N_R$  indicates the number of explicit regions and  $t_{CE}$  the time required by the certification algorithm on a 2.2 GHz Intel® Core i7-8750H. The results show that the so implemented implicit MP-TC is always faster and less eager in memory than explicit MPC, with the performance scaling more favorably for implicit MP-TC when increasing the horizon. Interestingly, explicit MP-TC is feasible only in two out of six configurations, namely the ones where the horizon is shortened with respect to the original setup, exceeding for the others both time and memory constraints. Implicit MP-TC is always feasible besides the single case of *Setup 1* with increased horizon. This not only proves the feasibility of CCS-MPC embedded on cheap hardware for motor control, but also that implicit MPC can be more efficient than explicit MPC even on a small problem.

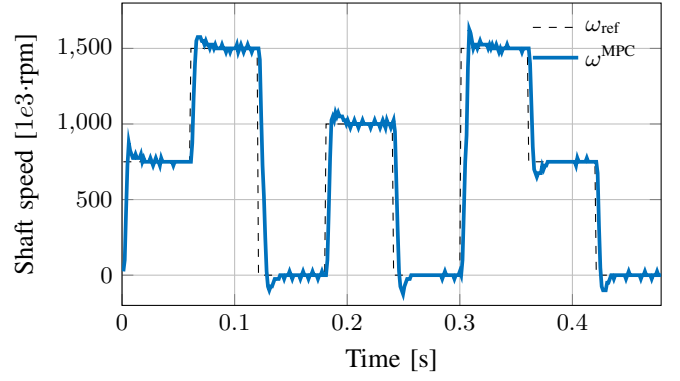


Figure 6. Speed tracking performance for MP-TC controller experimentally tested on MBE.300.E500 motor. Abrupt step changes in the reference shaft speed are applied to test the QP solver when constraints are active.

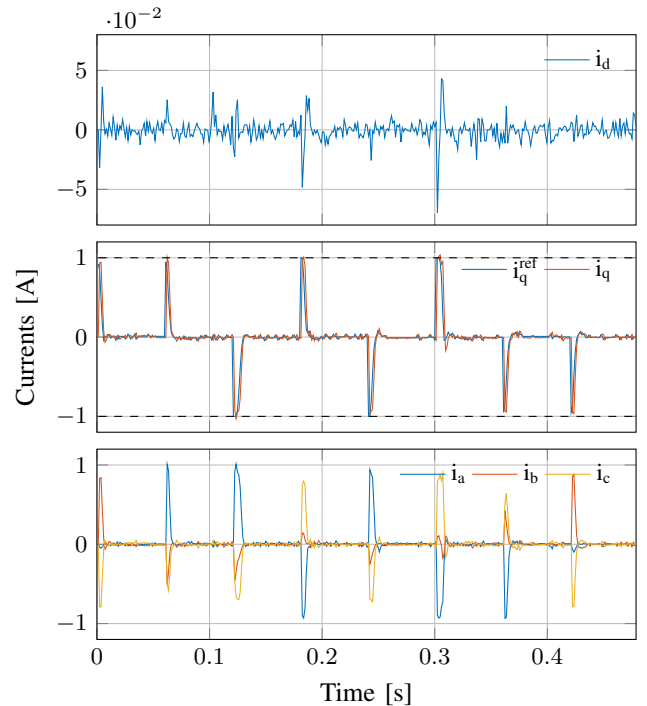


Figure 7. Stator currents for the experimental test of MP-TC controller. From top to bottom: *i*) stator current in the direct frame, *ii*) stator current in the quadrature frame (red), and the reference to track (blue), *iii*) three phase stator currents.

## VI. CONCLUSION

This paper has proposed a Model Predictive Torque Control (MP-TC) method with online optimization for permanent magnet synchronous motors. The optimal control inputs are obtained by solving a Quadratic Programming (QP) problem with an efficient, active-set, embedded solver. The computational complexity of the solver has been exactly assessed, fulfilling the mandatory requirement of worst-case time estimation for embedded control. We have shown that the proposed MP-TC with online solver is feasible on a control unit with scarce computational resources. The algorithm has been experimentally tested, and compared to explicit MPC which is considered so far one of the few options to implement MPC in motion

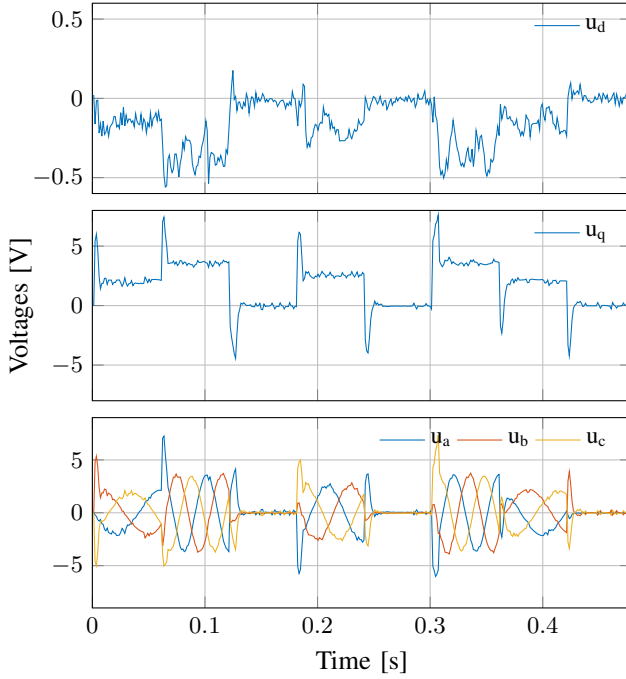


Figure 8. Stator voltages for the experimental test of MP-TC controller. From top to bottom: *i*) stator voltage in the direct frame, *ii*) stator voltage in the quadrature frame, *iii*) three phase stator voltages.

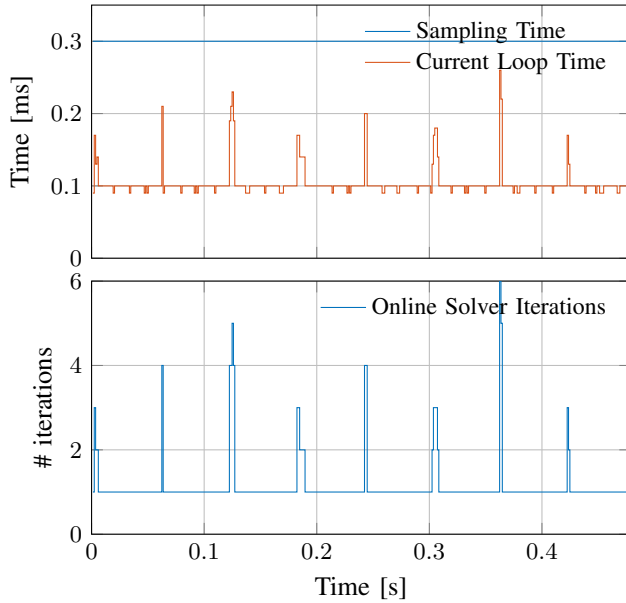


Figure 9. Timing performance of the F28335 DSP for the experimental test. From top to bottom: *i*) the time acquisitions of the control routine (red), compared to the time limit allowed (blue), *ii*) the number of iterations performed by the QP algorithm.

control. The results shows that the proposed QP solver not only saves considerable memory with respect to explicit MPC, but it is certified to be faster in the worst case, even if explicit MPC is implemented with an approximated formulation.

## REFERENCES

[1] P. Cortes, M. Kazmierkowski, R. Kennel, D. Quevedo, and J. Rodriguez, "Predictive Control in Power Electronics and Drives," *IEEE Transactions*

Table III  
PERFORMANCE BENCHMARK OF IMPLICIT AND EXPLICIT MP-TC WITH DIFFERENT PROBLEM SETUPS AND CONTROL PARAMETERS

$N_p$	Setup 1			Setup 2		
	2	3	4	2	3	4
<b>Implicit MP-TC</b>						
$m_I$ 32-bit [kB]	12.4	12.7	12.9	12.1	12.2	12.3
$\mathcal{F}_I^{\max}$ ( $\pm, *, \div$ ) sqrt	1932 10	2421 10	2904 10	944 7	1436 10	1598 10
$N_I^{\max}$	6	6	6	5	6	6
<b>Explicit MP-TC</b>						
$m_E$ 32-bit [kB]	31.1	50.9	62.8	21.8	36.6	45.6
$\mathcal{F}_E^{\max}$ ( $\pm, *$ )	2333	3868	4806	1740	2737	3812
$N_E$	82	133	163	54	95	119
$t_{CE}$ [s]	71.7	182.5	281.7	4.3	14.7	24.7

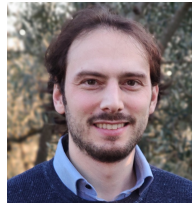
- on *Industrial Electronics*, vol. 55, no. 12, pp. 4312–4324, Dec. 2008.
- [2] H. Guzman, M. Duran, F. Barrero, B. Bogado, and S. Toral, "Speed Control of Five-Phase Induction Motors With Integrated Open-Phase Fault Operation Using Model-Based Predictive Current Control Techniques," *IEEE Transactions on Industrial Electronics*, vol. 61, no. 9, pp. 4474–4484, Sept 2014.
- [3] Y. Zhang, D. Xu, J. Liu, S. Gao, and W. Xu, "Performance Improvement of Model-Predictive Current Control of Permanent Magnet Synchronous Motor Drives," *IEEE Transactions on Industry Applications*, vol. 53, no. 4, pp. 3683–3695, July 2017.
- [4] S. Kouro, M. Perez, J. Rodriguez, A. Llor, and H. Young, "Model predictive control: MPC's role in the evolution of power electronics," *Industrial Electronics Magazine, IEEE*, vol. 9, no. 4, pp. 8–21, Dec 2015.
- [5] Z. Mynar, L. Vesely, and P. Vaclavek, "PMSM Model Predictive Control With Field-Weakening Implementation," *IEEE Transactions on Industrial Electronics*, vol. 63, no. 8, pp. 5156–5166, Aug 2016.
- [6] J. Rodriguez, M. Kazmierkowski, J. Espinoza, P. Zanchetta, H. Abu-Rub, H. Young, and C. Rojas, "State of the Art of Finite Control Set Model Predictive Control in Power Electronics," *IEEE Transactions on Industrial Informatics*, vol. 9, no. 2, pp. 1003–1016, May 2013.
- [7] M. Preindl and S. Bolognani, "Model Predictive Direct Torque Control With Finite Control Set for PMSM Drive Systems, Part 2: Field Weakening Operation," *IEEE Transactions on Industrial Informatics*, vol. 9, no. 2, pp. 648–657, May 2013.
- [8] A. A. Ahmed, B. K. Koh, and Y. I. Lee, "A Comparison of Finite Control Set and Continuous Control Set Model Predictive Control Schemes for Speed Control of Induction Motors," *IEEE Transactions on Industrial Informatics*, vol. PP, no. 99, pp. 1–1, 2017.
- [9] C.-S. Lim, E. Levi, M. Jones, N. Rahim, and W.-P. Hew, "A Comparative Study of Synchronous Current Control Schemes Based on FCS-MPC and PI-PWM for a Two-Motor Three-Phase Drive," *IEEE Transactions on Industrial Electronics*, vol. 61, no. 8, pp. 3867–3878, Aug. 2014.
- [10] F. Morel, X. Lin-Shi, J.-M. Retif, B. Allard, and C. Buttay, "A comparative study of predictive current control schemes for a permanent-magnet synchronous machine drive," *IEEE Transactions on Industrial Electronics*, vol. 56, no. 7, pp. 2715–2728, Jul. 2009.
- [11] H. T. Nguyen and J. Jung, "Disturbance-Rejection-Based Model Predictive Control: Flexible-Mode Design With a Modulator for Three-Phase Inverters," *IEEE Transactions on Industrial Electronics*, vol. 65, no. 4, pp. 2893–2903, April 2018.
- [12] T. Geyer, G. Papafotiou, and M. Morari, "Model Predictive Direct Torque Control - Part I: Concept, Algorithm, and Analysis," *IEEE Transactions on Industrial Electronics*, vol. 56, no. 6, pp. 1894–1905, Jun. 2009.
- [13] F. Mwasilu, E. K. Kim, M. S. Razaq, and J. W. Jung, "Finite Set Model Predictive Control Scheme with an Optimal Switching Voltage Vector Technique for High-Performance IPMSM Drive Applications," *IEEE Transactions on Industrial Informatics*, vol. PP, no. 99, pp. 1–1, 2017.
- [14] J. I. Metri, H. Vahedi, H. Y. Kanaan, and K. Al-Haddad, "Real-Time Implementation of Model-Predictive Control on Seven-Level Packed U-Cell Inverter," *IEEE Transactions on Industrial Electronics*, vol. 63, no. 7, pp. 4180–4186, July 2016.
- [15] M. R. Arahal, F. Barrero, M. J. Durán, M. G. Ortega, and C. Martín, "Trade-offs analysis in predictive current control of multi-phase induc-

tion machines,” *Control Engineering Practice*, vol. 81, pp. 105 – 113, 2018.

- [16] M. R. Arahal, C. Martin, F. Barrero, and M. J. Duran, “Assessing Variable Sampling Time Controllers for Five-Phase Induction Motor Drives,” *IEEE Transactions on Industrial Electronics*, pp. 1–1, 2019.
- [17] A. D. Alexandrou, N. K. Adamopoulos, and A. G. Kladas, “Development of a Constant Switching Frequency Deadbeat Predictive Control Technique for Field-Oriented Synchronous Permanent-Magnet Motor Drive,” *IEEE Transactions on Industrial Electronics*, vol. 63, no. 8, pp. 5167–5175, Aug 2016.
- [18] M. Preindl and S. Bolognani, “Model Predictive Direct Speed Control with Finite Control Set of PMSM Drive Systems,” *IEEE Transactions on Power Electronics*, vol. 28, no. 2, pp. 1007–1015, Feb. 2013.
- [19] L. Cavanini, G. Cimini, and G. Ippoliti, “Model predictive control for pre-compensated power converters: Application to current mode control,” *Journal of the Franklin Institute*, vol. 356, no. 4, pp. 2015 – 2030, 2019.
- [20] S. Rubino, R. Bojoi, S. A. Odhano, and P. Zanchetta, “Model Predictive Direct Flux Vector Control of Multi-three-Phase Induction Motor Drives,” *IEEE Transactions on Industry Applications*, vol. 54, no. 5, pp. 4394–4404, Sep. 2018.
- [21] D. E. Quevedo, R. P. Aguilera, and T. Geyer, *Model Predictive Control for Power Electronics Applications*. Cham: Springer International Publishing, 2019, pp. 551–580.
- [22] P. Karamanakos, T. Geyer, and R. P. Aguilera, “Long-Horizon Direct Model Predictive Control: Modified Sphere Decoding for Transient Operation,” *IEEE Transactions on Industry Applications*, vol. 54, no. 6, pp. 6060–6070, Nov 2018.
- [23] G. Cimini and A. Bemporad, “Exact Complexity Certification of Active-Set Methods for Quadratic Programming,” *IEEE Transactions on Automatic Control*, vol. 62, no. 12, pp. 6094–6109, Dec 2017.
- [24] A. Bemporad, M. Morari, V. Dua, and E. N. Pistikopoulos, “The explicit linear quadratic regulator for constrained systems,” *Automatica*, vol. 38, no. 1, pp. 3 – 20, 2002.
- [25] S. Bolognani, S. Bolognani, L. Peretti, and M. Zigliotto, “Design and Implementation of Model Predictive Control for Electrical Motor Drives,” *IEEE Transactions on Industrial Electronics*, vol. 56, no. 6, pp. 1925–1936, Jun. 2009.
- [26] J. Scoltock, T. Geyer, and U. Madawala, “A Comparison of Model Predictive Control Schemes for MV Induction Motor Drives,” *IEEE Transactions on Industrial Informatics*, vol. 9, no. 2, pp. 909–919, May 2013.
- [27] M. Preindl, S. Bolognani, and C. Danielson, “Model Predictive Torque Control with PWM using fast gradient method,” in *2013 Twenty-Eighth Annual IEEE Applied Power Electronics Conference and Exposition (APEC)*, Mar. 2013, pp. 2590–2597.
- [28] G. Cimini, D. Bernardini, A. Bemporad, and S. Levijoki, “Online model predictive torque control for Permanent Magnet Synchronous Motors,” in *Industrial Technology (ICIT), 2015 IEEE International Conference on*, March 2015, pp. 2308–2313.
- [29] A. Bemporad, D. Bernardini, R. Long, and J. Verdejo, “Model predictive control of turbocharged gasoline engines for mass production,” in *SAE Technical Paper*. SAE International, 04 2018.
- [30] A. Bemporad, D. Bernardini, M. Livshiz, and B. Pattipati, “Supervisory model predictive control of a powertrain with a continuously variable transmission,” in *SAE Technical Paper*. SAE International, 04 2018.
- [31] I. Necoara, “Computational complexity certification for dual gradient method: Application to embedded MPC,” *Systems & Control Letters*, vol. 81, pp. 49 – 56, 2015.
- [32] G. Cimini and A. Bemporad, “Complexity and convergence certification of a block principal pivoting method for box-constrained quadratic programs,” *Automatica*, vol. 100, pp. 29 – 37, 2019.
- [33] A. Damiano, G. Gatto, I. Marongiu, A. Perfetto, and A. Serpi, “Operating Constraints Management of a Surface-Mounted PM Synchronous Machine by Means of an FPGA-Based Model Predictive Control Algorithm,” *IEEE Transactions on Industrial Informatics*, vol. 10, no. 1, pp. 243–255, Feb. 2014.
- [34] A. Forsgren, P. E. Gill, and E. Wong, “Primal and dual active-set methods for convex quadratic programming,” *Mathematical Programming*, pp. 1–40, 2015.
- [35] H. J. Ferreau, H. G. Bock, and M. Diehl, “An online active set strategy to overcome the limitations of explicit MPC,” *International Journal of Robust and Nonlinear Control*, vol. 18, no. 8, pp. 816–830, 2008.
- [36] M. Baotić, F. Borrelli, A. Bemporad, and M. Morari, “Efficient On-Line Computation of Constrained Optimal Control,” *SIAM Journal on Control and Optimization*, vol. 47, no. 5, pp. 2470–2489, 2008.



**Gionata Cimini** received his Master’s degree in Computer and Automation Engineering in 2012 and his Ph.D. degree in Information Engineering, in 2017, from Università Politecnica delle Marche, Italy. He has been a guest Ph.D. scholar at IMT Alti Studi di Lucca, Italy, and a visiting Ph.D. scholar at University of Michigan, USA. He held research assistant positions at the Information Department, Università Politecnica delle Marche and at the Automotive Research Center, University of Michigan. In 2016, he was a contract employee at General Motors Company, USA. In 2017 he joined ODYS Srl, where he is currently the technical manager for numerical optimization. His research interests include model predictive control, embedded optimization, and their application to problems in the automotive, aerospace and power electronics domains.



**Daniele Bernardini** received his master’s degree in Computer Engineering in 2007 and his Ph.D. in Information Engineering in 2011 from the University of Siena, Italy, specializing in automatic control. In 2011–2015 he was with the Dynamical Systems, Control and Optimization (DYSCO) research unit at IMT Lucca as a post-doctoral fellow. In 2011 he co-founded ODYS Srl where he is CTO. His main expertise is in model predictive control and its industrial applications in the domains of automotive, aerospace, energy, and process control.



**Stephen P. Levijoki** holds a Bachelors of Science in Electrical Engineering from the University of Michigan, Ann Arbor, and a Master of Science in Systems Architecting and Engineering from the University of Southern California Viterbi School of Engineering. Mr. Levijoki holds 34 United States Patents and a 2018 General Motors Charles F. “Boss” Kettering award for Use of Model Predictive Control (MPC) in Gasoline Engines. He also is a recipient of the General Motors Research & Development Charles L. McCuen Special Achievement Innovation Award.



**Alberto Bemporad** received his Master’s degree in Electrical Engineering in 1993 and his Ph.D. in Control Engineering in 1997 from the University of Florence, Italy. In 1996/97 he was with the Center for Robotics and Automation, Department of Systems Science & Mathematics, Washington University, St. Louis. In 1997–1999 he held a postdoctoral position at the Automatic Control Laboratory, ETH Zurich, Switzerland, where he collaborated as a senior researcher until 2002. In 1999–2009 he was with the Department of Information Engineering of the University of Siena, Italy, becoming an Associate Professor in 2005. In 2010–2011 he was with the Department of Mechanical and Structural Engineering of the University of Trento, Italy. Since 2011 he is Full Professor at the IMT School for Advanced Studies Lucca, Italy, where he served as the Director of the institute in 2012–2015. He spent visiting periods at Stanford University, University of Michigan, and Zhejiang University. In 2011 he cofounded ODYS S.r.l., a company specialized in developing model predictive control systems for industrial production. He has published more than 350 papers in the areas of model predictive control, hybrid systems, optimization, automotive control, and is the co-inventor of 16 patents. He is author or coauthor of various MATLAB toolboxes for model predictive control design, including the Model Predictive Control Toolbox (The Mathworks, Inc.) and the Hybrid Toolbox. He was an Associate Editor of the IEEE Transactions on Automatic Control during 2001–2004 and Chair of the Technical Committee on Hybrid Systems of the IEEE Control Systems Society in 2002–2010. He received the IFAC High-Impact Paper Award for the 2011–14 triennial and the IEEE CSS Transition to Practice Award in 2019. He is an IEEE Fellow since 2010.